Carbohydrate Polymers 267 (2021) 118157

Contents lists available at ScienceDirect

Carbohydrate Polymers

journal homepage: www.elsevier.com/locate/carbpol

Quercetin delivery characteristics of chitosan nanoparticles prepared with different molecular weight polyanion cross-linkers

Eun Suh Kim [1], Da Young Kim [1], Ji-Soo Lee, Hyeon Gyu Lee [*]

Department of Food and Nutrition, Hanyang University, 222, Wangsimni-ro, Seongdong-gu, Seoul 04763, Republic of Korea

ARTICLE INFO

Keywords:
Nanoencapsulation
Chitosan
Cross-linker
Mucoadhesion
Cell permeability
Antioxidant activity

ABSTRACT

The aim of the study was to investigate the effects of cross-linkers on quercetin (QUE) absorption characteristics of QUE-loaded chitosan nanoparticles (CS-NPs). CS-NPs (461.2–482.7 nm) were prepared by ionic gelation at pH 3.5 using tripolyphosphate (367.9 Da), dextran sulfate (>15 kDa), arabic gum (AG, >250 kDa), or hyaluronic acid (HA, >1000 kDa). Mucoadhesion and cell permeation of QUE were significantly increased by positive charged CS-NPs due to interactions with negatively charged mucosal layer. Moreover, CS-AG and CS-HA NPs prepared with relatively higher MW cross-linkers exhibited significantly higher adhesion and permeation than the others. These results were verified by a cellular antioxidant activity assay; CS-AG (137.5 unit) and CS-HA NPs (126.5 unit) showed significantly higher activities after internalization into Caco-2 cells. Therefore, encapsulation within CS-NPs prepared using high MW cross-linkers such as AG and HA is found to be potentially valuable techniques for improving the QUE absorption.

1. Introduction

Quercetin (QUE), the major representative of the flavonol subclass of flavonoids is ubiquitously present in vegetables and fruits as well as countless food supplements (Boots et al., 2008). It has been recognized for having beneficial clinical properties, specifically antioxidative activities through several mechanisms, such as scavenging oxygen radicals, protecting against lipid peroxidation, and chelating metal ions (Coskun et al., 2005). However, low extent of intestinal absorption of QUE is known to as the critical drawback for its oral administration (Hollman et al., 1997; Murota & Terao, 2003). To overcome the drawbacks of food compounds with this kind of problem, nanoencapsulation techniques have been applied as the promising solution (Caddeo et al., 2016).

Nanoencapsulation is defined as a technology to entrapped one substance with the other wall materials, and refers to comprising the manufacture, processing, and application of materials at the nanometer scale (Sanguansri & Augustin, 2006; Sozer & Kokini, 2009). Since the most distinct feature of nanoencapsulation is the ability to modify the physicochemical and biological properties of materials by increasing surface area through size-reduction, it has been used for bioactive materials to enhance absorption and delivery through the gastrointestinal tract (Dan, 2016). Among the various methods for nanoencapsulation, chitosan nanoparticles (CS-NPs) prepared by ionic gelation technique is one of the primary method for food industry due to its economic feasibility, simplicity, and non-toxicity (Nurunnabi et al., 2017; Racoviţă et al., 2009).

CS, a natural polysaccharide derived by deacetylation of chitin found in crab has a cationic charge in acidic aqueous solution due to the abundance of positively charged amino groups. Because of its positive charge, CS can cross-link with oppositely charged ingredients through electrostatic interaction, and form gel NPs effectively in the presence of polyanion cross-linkers (Luo & Wang, 2013). Encapsulation technology based on CS-NPs has been applied to various bioactive substances such as catechin, ascorbic acid, and resveratrol to improve their stability against acidic environments including heat and UV light, and gastrointestinal environment after oral administration led to efficient storage and gastrointestinal delivery (Jang & Lee, 2008; Wu et al., 2017). Moreover, CS-NPs have attracted much interest as delivery system due to the numerous advantages that positively charged CS-NPs can exhibit a stronger affinity toward negatively charged cell membranes, resulting in increased mucoadhesion and cell permeability (Liang et al., 2017).

Recent studies about CS-NPs have been explored the various factors for enhancing biodelivery characteristics. CS was synthesized in the

* Corresponding author.
E-mail address: hyeonlee@hanyang.ac.kr (H.G. Lee).
[1] These authors contributed equally to this work.

https://doi.org/10.1016/j.carbpol.2021.118157
Received 4 January 2021; Received in revised form 29 March 2021; Accepted 15 April 2021
Available online 7 May 2021

form of trimethyl chitosan chloride (TMC), the partially quaternized derivative of CS for enhancing mucoadhesion and permeation of insulin during oral administration (Yin et al., 2009). Moreover, effects of molecular weight (MW) of CS on characteristics of CS-NPs such as encapsulation efficiency and *in vitro* release properties were analyzed (Yang & Hon, 2009). Also, the influence of particle size of CS-NPs on the intestinal cellular absorption of resveratrol entrapped within CS-NPs was investigated (Je et al., 2017). However, only few studies have directly compared the biodelivery characteristics of CS-NPs according to type of cross-linker (Raja et al., 2015).

Polyanion cross-linkers for fabricating CS-NPs can be classified according to functional group, namely, phosphate (PO_4), carboxyl (COOH), and sulfate (SO_4) (Kim & Shin, 2015). Tripolyphosphate (TPP) with a phosphate group has been widely used as a cross-linker, whereas the use of cross-linkers containing carboxyl or sulfate groups is more recent (Luo & Wang, 2014). CS-NPs prepared using the representative carboxylated cross-linkers arabic gum (AG) and hyaluronic acid (HA) and the sulfated cross-linker dextran sulfate (DS) exhibited enhanced stability, bioactivity, cell permeability, and sustained release of bioactive compounds such as polyphenols (Lee et al., 2017; Shim et al., 2016; Yang et al., 2015). Since CS-NPs are fabricated by ionic gelation between CS and oppositely charged cross-linkers, we hypothesized that encapsulation and biodelivery properties of CS-NPs can be significantly influenced by the characteristics of cross-linkers (Agnihotri et al., 2004; Ramasamy et al., 2014). Moreover, a comparative study of CS-NPs prepared by various cross-linkers under constant experimental conditions can be expected to effectively reveal the effect of cross-linkers on CS-NPs properties.

Therefore, the aim of this study was to analyze the effects of cross-linker on the biodelivery characteristics of CS-NPs, and to investigate the effective CS-NPs formulations for improving QUE absorption. QUE-loaded CS-NPs were fabricated using either TPP, DS, AG, and HA were analyzed for their physicochemical properties of particle size, zeta potential (ZP), polydispersity index (PDI), encapsulation efficiency (EE), loading efficiency (LE), and *in vitro* release properties. Moreover, the effects of CS-NPs according to the type of cross-linker on biodelivery of QUE were analyzed by *in vitro* mucin adhesion, intestinal cell permeability, *in vitro* 1,1-diphenyl-2-picrylhydrazyl (DPPH) radical scavenging, and cellular antioxidant activities assay.

2. Materials and methods

2.1. Materials

Chitosan (CS, 50–190 kDa, 24 cps, 95% deacetylated), Tripolyphosphate (TPP, 367.9 Da), arabic gum (AG, >250 kDa), dextran sulfate (DS, 15 kDa), quercetin (QUE, ≤95%), and mucin (extracted from porcine stomach, type III) were purchased from Sigma-Aldrich Co. (St. Louis, MO, USA). Hyaluronic acid (HA, >1000 kDa) was purchased from Bioland (Cheonan, South Korea). All other chemicals were of reagent grade, and all solvents were of HPLC grade. Colon carcinoma (Caco-2) and human colon tumor (HT-29) cells were purchased from the Korean Cell Line Bank (KCLB, Seoul, South Korea). Dulbecco's Modified Eagle's culture medium (DMEM), non-essential amino acid (NEAA), fetal bovine serum (FBS), Hank's balanced salt solution (HBSS), and 0.25% trypsin-EDTA were purchased from Gibco Invitrogen Co. (Grand Island, NY, USA). Phosphate-buffered saline (PBS) and penicillin−streptomycin were purchased from Lonza (Walkersville, MD, USA).

2.2. Conductivity investigation

CS and cross-linkers were dissolved in 2% (*v*/v) acetic acid aqueous solution and distilled water to a concentration of 1 mg/mL, respectively under magnetic stirring conditions (MS-MP8, Daihan Co., Seoul, Korea, 500 rpm). All solutions were pH-adjusted from 2 to 7 as indicated using 1 N HCl or NaOH solution. Finally, pH adjusted solutions were transferred into a DTS 1060 cell, and conductivity was measured using a Zetasizer Nano ZS (Malvern Instruments Ltd., Worcestershire, UK) (Butstraen & Salaün, 2014).

2.3. Preparation of QUE-loaded CS-NPs

QUE-loaded CS-NPs were prepared by the ionic gelation method (Jang & Lee, 2008). Briefly, CS was dissolved in 2% (*v*/v) acetic acid to a final concentration of 0.75 mg/mL, and the cross-linkers of TPP, DS, AG, and HA were dissolved separately in DW to final concentrations of 2.18, 1.5, 6.0, and 6.0 mg/mL, respectively. Each of the initial solutions was adjusted to pH 3.5 using 1 N HCl or NaOH. Next, 5 mL of the CS solution was mixed with 1.5 mL of QUE (300 μM, dissolved in 50% (v/v) ethanol) under magnetic stirring at 1200 rpm for 10 min, followed by addition of 1 mL of a cross-linker solution. Continuous stirring of the mixture led to the immediate formation of QUE-loaded CS-NPs. The final concentration of each component is shown in Table 1.

2.4. Characterization of CS-NPs

Mean particle size, PDI, and ZP of CS-NPs were assessed by dynamic light scattering (DLS) using a Zetasizer Nano ZS. QUE-loaded CS-NPs suspension obtained immediately after fabrication were subjected to Zetasizer using appropriate vial, and measurements were performed at multiple narrow modes at 25 ± 1 °C.

2.5. Morphological properties of CS-NPs

The morphological properties of the nanoparticles were investigated by high-resolution transmission electron microscopy (TEM, JEM 2100F, Jeol, Tokyo, Japan). The nanoparticle suspension was dropped onto a 200-mesh copper-carbon-film TEM grid and air-dried at 37 °C. The dried samples were stained for 30 min using a 2% phosphotungstic acid solution before TEM observation.

2.6. QUE determination

QUE was quantified using a Waters 1525 high-performance liquid chromatography (HPLC) system consisting of a Waters 2487 UV absorbance detector (Waters Corp., Milford, MA, USA) (Kim et al., 2012). Each sample (100 μL) was injected onto an XDB C18 column (4.6 × 150 mm, 5 μm, Agilent Technology, Wilmington, DE, USA), and separation was carried out using an isocratic elution system consisting of DW/5% (*v*/v) acetic acid/acetonitrile (40:30:30, v/v/v). The flow rate was set to 1 mL/min, and the sample was detected at an ultraviolet (UV) wavelength of 370 nm. QUE concentrations were determined using a standard curve obtained from HPLC peaks of commercial standards.

2.7. Encapsulation and loading efficiencies

QUE-loaded CS-NP suspensions were ultra-centrifuged (27,600 ×*g* at 4 °C) for 30 min (Optima TL, Beckman Instruments, Fullerton, CA, USA). Next, unencapsulated QUE present in the supernatant was quantified using the HPLC system after filtration through a 0.45 μm pore size membrane filter. EE and LE were calculated using the following equations, respectively (Kumari et al., 2010).

$$\text{EE}\ (\%) = \frac{\text{Actual amount of QUE in CS} - \text{NPs}}{\text{Theoretical amount of QUE in CS} - \text{NPs}} \times 100 \quad (1)$$

$$\text{LE}\ (\%) = \frac{\text{Actual amount of QUE in CS} - \text{NPs}}{\text{Total amount of QUE} - \text{loaded CS} - \text{NPs}} \times 100 \quad (2)$$

2.8. In vitro release properties

Briefly, simulated gastric (SGF) and intestinal fluid (SIF) were pre-

Table 1
Preparation conditions and characteristics of quercetin-loaded chitosan nanoparticles prepared with different cross-linkers.

Types of nanoparticles	Chitosan (mg/mL)	Quercetin (μM)	Cross-linker (mg/mL)	Particle size (nm)	Polydispersity index	Zeta potential (mV)	Encapsulation efficiency (%)	Loading efficiency (%, w/w)
CS-TPP NPs	0.5	60	0.29[1]	461.2 ± 13.1	0.293 ± 0.050	14.8 ± 1.6[d]	48.7 ± 0.4[c]	1.11 ± 0.01[c]
CS-DS NPs			0.20[2]	468.1 ± 38.0	0.337 ± 0.091	34.1 ± 1.3[a]	98.3 ± 0.7[a]	2.48 ± 0.02[a]
CS-AG NPs			0.80[3]	482.7 ± 22.7	0.350 ± 0.071	31.2 ± 1.2[b]	94.8 ± 0.8[ab]	1.31 ± 0.01[b]
CS-HA NPs			0.80[4]	462.4 ± 38.5	0.295 ± 0.039	19.6 ± 1.1[c]	92.5 ± 2.7[b]	1.27 ± 0.04[b]

[a–d]Different letters in the same column indicate significant differences ($p < 0.05$).
[1] Tripolyphosphate.
[2] Dextran sulfate.
[3] Arabic gum.
[4] Hyaluronic acid.

pared using 0.05 M sodium chloride adjusted to pH 1.2 with 1 N HCl, and 0.05 M sodium dihydrogen phosphate buffer adjusted to pH 6.8 with 1 N NaOH, respectively (Abd El-Ghaffar et al., 2012). Suspensions of QUE-loaded CS-NPs obtained immediately after preparation (10 mL) were then added to dialysis membranes (MW cut off 8–10 kDa, Biotech RC membrane, Spectrum Laboratories, CA, USA). Membranes containing the solution to be dialyzed were then placed into SGF (70 mL) for 2 h and were continuously transferred into SIF for 2–8 h under magnetic stirring at 80 rpm. Samples of QUE released from CS-NPs were collected (1 mL) from the dissolution medium at the appropriate time points and replenished with respective fresh medium. QUE was analyzed by the HPLC as described above, and the QUE release rate was calculated using the following equation (Bagre et al., 2013).

$$\text{Release rate } (\%) = \frac{\text{Amount of QUE released from CS} - \text{NPs}}{\text{Amount of QUE initially entrapped in CS} - \text{NPs}} \times 100 \quad (3)$$

2.9. In vitro mucoadhesion assay

Briefly, 0.6 mL of a mucin solution (0.5 mg/mL) was mixed with 0.6 mL of free QUE or QUE-loaded CS-NPs and then incubated at 37 °C for 1 h with shaking (J-USR, Jisico Co., Seoul, South Korea). The mixture was centrifuged at 9400 ×*g* for 5 min, and the amount of free mucin in the supernatant was measured by Bradford assay (Compton & Jones, 1985). The supernatant was then incubated with Bradford reagent for 5 min, after which the UV absorbance at 595 nm was measured with a Synergy HT multi-microplate reader (BioTek Instruments, Winooski, VT, USA). The amount of mucin attached to QUE or QUE-loaded CS-NPs was calculated as the difference between the total amount of added mucin and the free mucin content in the supernatant (Lee et al., 2017).

2.10. Preparation of cell monolayers

The Caco-2 and HT-29 cells used in this study were between passages 23-50 and 8-31, respectively. Caco-2 and HT-29 cells were grown separately in DMEM (supplemented with 10% FBS, 5% NEAA, and 5% penicillin-streptomycin) and maintained at 37 °C with 5% CO_2 and 95% humidity (BB 15, Thermo Scientific, Waltham, IL, USA) (Antunes et al., 2013). The medium was changed every 2 days. Upon reaching confluency, each cell type was mixed prior to seeding to yield a cell ratio of Caco-2 to HT-29 cells of 9:1. The cells were co-cultured in DMEM containing 10% FBS, 1% NEAA, and 1% penicillin-streptomycin and incubated at 37 °C with 5% CO_2 and 95% humidity. Co-cultures were harvested with trypsin-EDTA and seeded at a density of 1.5×10^5 cells/cm^2 on polycarbonate filters of transwell cell culture chamber (0.4 μm pores, 1.22 cm^2 growth area, Corning Inc., Corning, NY, USA). Cultures were grown for approximately 21 days, with medium replaced every other day. To monitor the integrity of the cell monolayer, transepithelial electrical resistance (TEER) values across the cell monolayer were measured using an EVOM volt ohmmeter (World Precision Instruments, Sarasota, FL, USA), and only cultures with a TEER value of 400–500 Ω cm^2 were used for cell permeability studies (Je et al., 2017).

2.11. Cell permeability assay

For cell permeability analysis, inserts containing monolayers were washed twice with HBSS (pH 7.4, supplemented with 25 mM glucose and 25 mM HEPES) and incubated at 37 °C for 30 min after the apical and basolateral chambers of each well were filled with 0.5 and 1.5 mL of fresh medium, respectively. Next, media in the apical and basolateral chambers were replaced with a suspension of free QUE or QUE-loaded CS-NPs (0.5 mL) and HBSS (1.5 mL), respectively. Inserts containing monolayers were then transferred to different wells with fresh medium every 30 min; the transwell plate was continuously shaken at 60 rpm throughout the assay (J-USR; Jisico Co., Seoul, South Korea). The amount of free QUE representing QUE-loaded CS-NPs transported across the monolayer was determined by performing HPLC on the medium obtained from each well. The apparent permeability coefficient (P_{app}) was calculated using the following equation (Je et al., 2017).

$$P\text{app } (\text{cm/s}) = (dQ/dt) \times 1/(A \times C0) \times 1/60 \quad (4)$$

where dQ/dt is the transport flux of QUE across the monolayer, A is the surface area of the membrane, and C0 is the initial RV concentration in the apical chamber. The transport flux across the monolayer was calculated from the slope of the cumulative amount of RV transported to the basolateral chamber. Each transport assay was conducted in triplicate.

2.12. In vitro DPPH radical scavenging activity

Suspensions of free QUE and QUE-loaded CS-NPs (100 μL) were added to 50 μM DPPH in ethanol (100 μL) in 96-well plates. After incubation for 45 min at 25 °C in darkness, the absorbance of the resulting solution was determined at 517 nm with a Synergy HT Multi-microplate reader. DPPH scavenging activity was calculated using the following equation (Brand-Williams et al., 1995).

$$\text{DPPH radical scavenging activity } (\%) = \frac{(C - CB) - (S - SB)}{C - CB} \times 100 \quad (5)$$

where C, CB, S, and SB are the absorbance values of the control, control blank, sample, and sample blank, respectively.

2.13. Cellular antioxidant activity

Caco-2 cells were seeded at a density of 6×10^4 cells/well in a black 96-well plate for fluorescence measurements in 100 μL of growth medium/well. After incubation for 24 h, growth medium was removed, and the wells were washed with 100 μL of PBS. Next, the wells were treated with 50 μL of either free QUE or QUE-loaded CS-NPs, to which 50 μL of a 25 μM solution of dichloro-dihydro-fluorescein diacetate (DCFH-DA) dissolved in HBSS medium was added. After incubation for 1 h, the wells were washed with 100 μL of PBS and treated with 600 μM of 2,2′-azobis

(2-amidinopropane) dihydrochloride (ABAP) dissolved in HBSS (100 μL). The fluorescence intensity of each well was measured every 5 min for 1 h with a Synergy HT multi-microplate reader (excitation 485 nm and emission 538 nm), and the cellular antioxidant activity unit was calculated using the following equation (Wan et al., 2015).

$$\text{CAA unit} = 100 - \left(\int SA \Big/ \int CA \right) \times 100 \quad (6)$$

where ∫SA is the integrated area under the sample fluorescence *versus* time curve, and ∫CA is the integrated area from the control curve.

2.14. Statistical analysis

All data are expressed as the mean ± standard deviation (SD) of triplicate experiments. Statistical analysis was performed using one-way ANOVA followed by Duncan's multiple range test (SPSS Version 21.0, SPSS Inc., Chicago, IL, USA). *P*-values below 0.05 were considered statistically significant.

3. Results and discussion

3.1. Conductivity

Conductivity is the mobility or concentration of ions in a solution and can be influenced by the binding of residual ions to functional groups of polymers dispersed in solutions (Butstraen & Salaün, 2014). Moreover, it is possible to anticipate the change in degree of protonation and ionization of the polymer based on the change in conductivity (Kizilay et al., 2011). When CS dissolves in a solution of acetic acid, the amino groups (NH_2) of CS convert to a positive charge (NH_3^+) due to the binding of hydrogen ions (H^+) (Jang & Lee, 2008). Likewise, when cross-linkers dissolved in DW, their phosphate (PO_4), sulfate (SO_2), and carboxyl (COOH) groups dissociate the H^+ ions, resulting in the formation of water after binding to hydroxide ions (OH^-), and are subsequently converted to PO_3^-, SO^-, and COO^-, respectively (Akahane et al., 1990). Therefore, an increase in protonated CS and deprotonated cross-linkers can increase the binding of liberated H^+ and OH^- ions, respectively, leading to a decrease in conductivity since the abundance of free ions in the solution decreases.

The conductivity of a CS solution decreased from 2.11 to 0.10 s/m as the pH increased from 1.58 to 3.06, and the values increased steadily as the pH increased from 3.06 to 7.07 (Fig. 1). On the other hand, the conductivity of cross-linkers decreased as the pH increased to 3.5 regardless of the type, and was maintained below 0.05 at above pH 3.5.

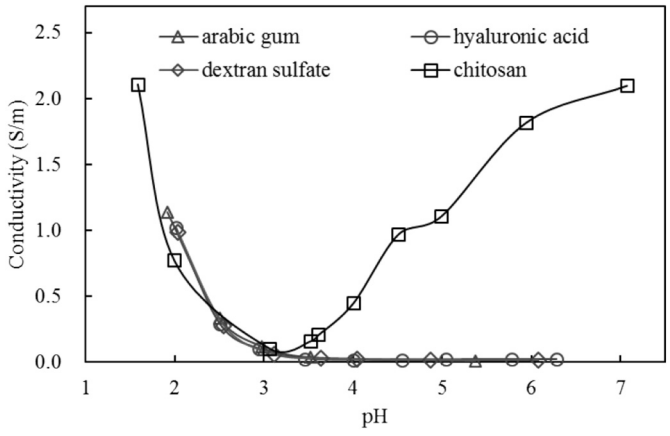

Fig. 1. Variation of electrolytic conductivity of wall materials according to pH values. Arabic gum, hyaluronic acid, and dextran sulfate were dissolved in distilled water and chitosan were dissolved in acetic acid (2%, *v*/v). Each wall material concentration was 1 mg/mL.

As mentioned above, it can be assumed that ionization of CS and cross-linker solutions is maximized at a pH range from 3.0 to 3.6 and above 3.5, respectively, where conductivity is the lowest. Since the CS-NPs were prepared by ionic gelation based on the electrostatic attraction between oppositely charged materials, increased protonation and ionization of cationic CS and anionic cross-linkers likely increased the efficiency of CS-NPs production due to an increase in the number of binding sites and attraction (Fan et al., 2012). Therefore, before preparation of CS-NPs for further experiments, CS and cross-linker solutions were adjusted to a pH of 3.5, which was associated with low conductivity of both.

3.2. Characteristics of QUE-loaded CS-NPs

Preliminary studies were conducted to determine the preparation conditions for QUE-loaded CS-TPP, -DS, -AG, and -HA NPs. As the CS-NPs were formed by ionic gelation between CS and charged cross-linkers, the characteristics of the NPs prepared by identical CS conditions were strongly influenced by the relative proportions, types, and properties of cross-linker used (Fan et al., 2012). Therefore, the concentration ranges of each cross-linker to fabricate CS-NPs of acceptable characteristics were primary determined based on particle size and PDI value. Particle size is the primary determinant of NPs characteristics. Conventionally, only particles with a size less than 100 nm can be claimed as NPs. However, the size range of NPs in the biomedical and food fields has been extended to 1000 nm. Especially, because processes and materials to satisfy food-grade safety concerns has resulted in the use of relatively low purity and large MW natural wall materials, which in turn has disrupted the ability to fabricate NP of small size, compared to the other fields (Je et al., 2017). PDI value is another critical factor indicative of particle size distribution. Specifically, lower PDI values indicate higher homogeneity, with values less than 0.1 indicating a monodisperse status and values greater than 0.7 indicating polydispersity. Within these ranges, NPs with PDI values less than 0.4 are generally considered to be nearly monodisperse and of acceptable size uniformity (Nidhin et al., 2008).

Under the constant concentration of QUE (60 μM) and CS (0.5 mg/mL), CS-TPP, -DS, -AG, and -HA NPs with acceptable PDIs were effectively prepared with particle sizes of 116–461, 375–452, 256–427, and 350–563 nm at the concentrations of TPP, DS, AG, and HA of 0.26–0.29, 0.10–0.30, 0.80–2.20, and 0.20–1.00 mg/mL, respectively. Since the aim of the study was to analyze of characteristics of CS-NPs according to type of polyanion cross-linker, each type of QUE-loaded CS-NP of the same particle size was selected within the concentration range of cross-linker where NPs were effectively fabricated (Table 1). Specifically, all QUE-loaded CS-NPs were fabricated with a particle size range of 461.2–482.7 nm and PDI values less than 0.4 without significant difference, confirming that each CS-NP within that size range was uniformly formed.

The particle sizes of CS-NPs were verified with the TEM micrograph (Fig. 2). QUE-loaded CS-NPs generally exhibited amorphous forms with size of approximately 400 nm. Particle size differences between the results of DLS and TEM can be explained that TEM micrograph were viewed in actual diameter of NPs in dry state while DLS evaluates hydrodynamic diameter of NPs (Fan et al., 2012). Moreover, TEM micrographs of CS-NPs with darker color toward to center demonstrated that the ionic gelation density was higher at the core region of CS-NPs.

ZP can be defined as the electric potential of the interfacial double layer of a particle or droplet dispersed in the continuous phase (Zhang et al., 2008). Since inter-particle repulsive forces in colloidal dispersions occur due to particle surface charges, the absolute ZP value of NPs can be used to ensure colloidal stability. In general, ZP values over 25 ± 5 mV are consistent with an ability to maintain a stable dispersion status for longer periods of time, while NPs with low ZP values may coagulate or flocculate during storage due to weak repulsion (Agnihotri et al., 2004). The ZP values of CS-TPP and CS-HA NPs were 14.8 and 19.6 mV,

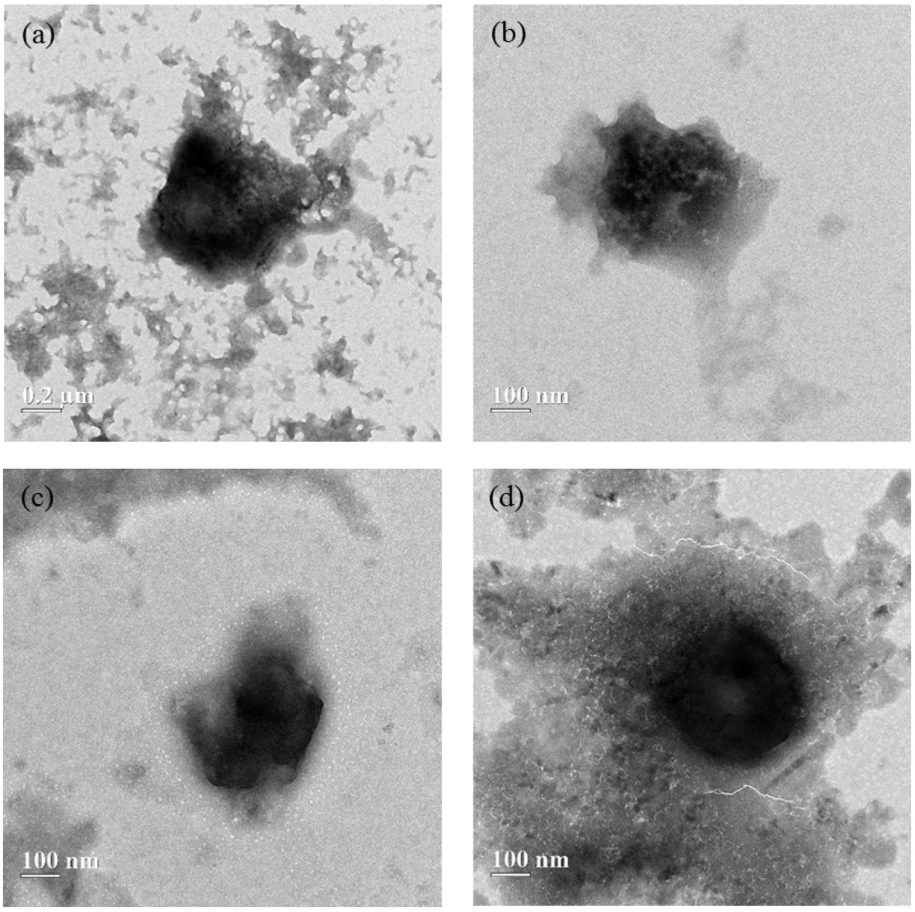

Fig. 2. TEM microscopic images of QUE-loaded CS-NPs prepared with (a) tripolyphosphate (TPP), (b) dextran sulfate (DS), (c) Arabic gum (AG), and (d) hyaluronic acid (HA). The suspension of QUE-loaded CS-NPs were deposited on copper-carbon grids and dried overnight at 37 °C. The dried QUE-loaded CS-NPs were stained for 30 min with a 2% phosphotungstic acid solution before TEM observation.

respectively, while the other NPs had ZP values greater than 30 mV. Therefore, CS-DS and CS-AG NPs were considered to be stable for relatively longer periods compared with CS-TPP and -HA NPs.

3.3. Encapsulation and loading efficiencies

The QUE EE of CS-TPP NPs was 48.7 ± 0.4%, while the other CS-NPs showed significantly higher EE ranging from 92.5 to 98.3%. The MW of TPP is approximately 367 Da (Jang & Lee, 2008), while the MWs of the other cross-linkers were much higher, consistent with branched-chain biopolymers. Specifically, DS consists of repeating D-glucose units with two to three sulfate groups (Lee et al., 2017), AG consists of β-galactopyranose units terminating in glucuronic acid (Shim et al., 2016) and HA consists of a disaccharide repeat unit of sodium glucuronate and *N*-acetylglucosamine (Yang et al., 2015). A previous study reported that use of alginate as a cross-linker for CS-NPs was associated with significantly higher EE compared with TPP, that denser structure of the NPs prepared with higher MW cross-linker attributed to entrap the core material more effectively (Akolade et al., 2017). Thus, it can be inferred that QUE was effectively encapsulated within the CS-NPs prepared using the cross-linkers other than TPP.

The results of the LE analyses were relevant to EEs, in that the QUE LE of CS-TPP NPs was 1.11 ± 0.01% (*w*/w), while those of the other CS-NPs were significantly higher, ranging from 1.27 to 2.48% (w/w). LE is proportional to the amount of bioactive compounds in the unit particles; thus, the low amount of QUE initially added for preparation of CS-NPs was generally thought to have been the reason for the low LE in this study. Specifically, the QUE concentration of 60 μM used to prepare CS-NPs in this study was determined based on a preliminary analysis of the cytotoxicity of QUE in Caco-2 and HT-29 co-cultured cells, since the cell viability decreased below 80% at concentrations of QUE greater than 60 μM (data not shown).

3.4. In vitro release properties

All of the CS-NPs exhibited similar QUE release behavior, in that QUE was gradually released for 8 h without burst release in response to an acidic pH environment and reached a plateau that was maintained through the end of the incubation period (Fig. 3). The charge intensity of materials is pH-dependent; thus, ionic gelation strength derived from opposite charge degrees can be influenced by the change in pH of the dispersion (Shu et al., 2001). Therefore, the electrostatic attraction between CS and each of the cross-linker may have weakened at SGF (pH 1.2) and SIF (pH 6.8), where the pH was lower or higher than the pH 3.5 of CS-NPs according to the parameters of the conductivity experiment. Weakening of ionic gelation also led to physicochemical degradation of the NP structures, resulting in a release of QUEs from the CS-NPs (Mounsey et al., 2008). When compared to CS-NPs according to cross-linker, CS-TPP NPs showed the highest QUE release rate, followed in decreasing order by CA-HA, -AG, and -DS NPs. As mentioned above, DS, AG, and HA are branched-chain structured polymers capable of fabricating denser CS-NP structures compared to TPP. Therefore, CS-NPs prepared using these cross-linkers appeared to experience prolonged degradation of the physicochemical properties of their respective NP structures and, as a result, had a generally higher degree of sustained QUE release.

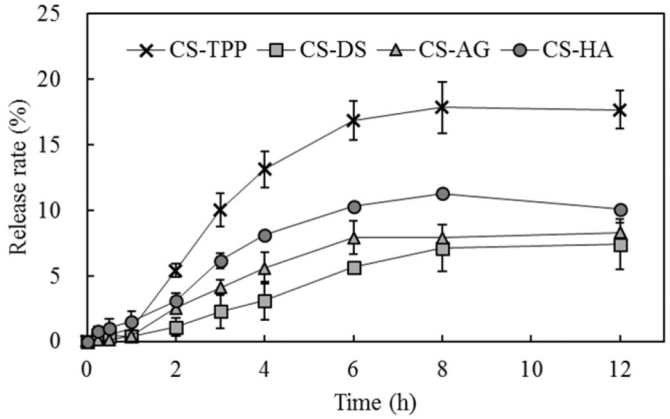

Fig. 3. *In vitro* release rate of QUE from CS-NPs prepared with tripolyphosphate (TPP), dextran sulfate (DS), Arabic gum (AG), and hyaluronic acid (HA) in simulated gastric fluid (pH 1.2) for 0–2 h and simulated intestinal fluid (pH 6.8) for 2–12 h. Data are the mean of three replicates, and error bars indicate the standard deviation.

3.5. *In vitro* mucoadhesion

The amount of mucin attached to free QUE was 0.05 mg/mL, and this amount was significantly increased by encapsulation within all types of CS-NPs (Fig. 4). Mucin, a high MW glycoprotein produced by epithelial tissues covering the mucosa plays several important biological roles in gastrointestinal protection, primarily by acting as a barrier to control permeation of bioactive materials (Suh et al., 2016). Therefore, prolonging the residence time of the bioactive materials on the mucosal layer can provide an effective means to increase their intestinal absorption and bioavailability during migration along the gastrointestinal tract. Moreover, since mucin forms a negatively charged aqueous gel bed on the epithelium surface, adhesion and permeation of positively charged materials can be accelerated due to electrical attraction. As mentioned above, CS-NPs are positively charged due to the amino groups of CS, and their cationic characteristics were confirmed by the ZP results. Therefore, the significant increase in attachment of QUE to mucin can be explained by the positively charged CS-NPs enhancing the electrostatic interactions with negatively charged mucin, resulting in increased adsorption (Lee et al., 2017).

A comparison across the different cross-linkers showed that CS-NPs prepared from carboxylic cross-linkers, namely, CS-AG (0.44 ± 0.02 mg/mL) and CS-HA NPs (0.50 ± 0.03 mg/mL), had significantly higher

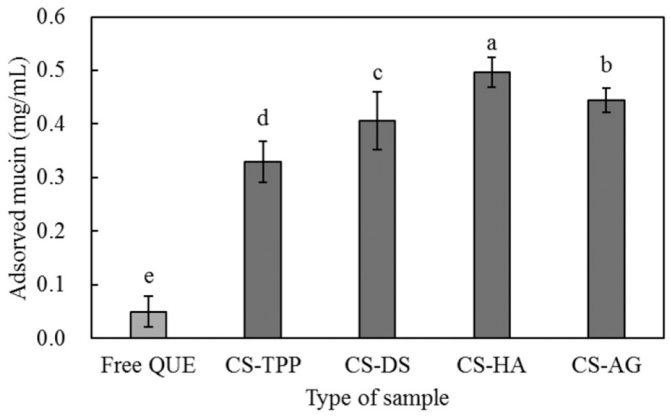

Fig. 4. *In vitro* mucin adhesiveness of the free QUE and QUE from CS-NPs prepared with tripolyphosphate (TPP), dextran sulfate (DS), Arabic gum (AG), and hyaluronic acid (HA). Data are the mean of three replicates, and error bars indicate the standard deviation. [a–e]Means with different letters indicate significant difference ($p < 0.05$).

mucoadhesion compared with CS-DS (0.41 ± 0.05 mg/mL) and CS-TPP NPs (0.33 ± 0.04 mg/mL), with CS-HA NPs exhibiting the highest degree of mucoadhesion by a significant margin. These results can also be explained in terms of MW rather than other influencing factors for mucoadhesion such as concentration and material charge (Salamat-Miller et al., 2005). Specifically, the adhesive strength of polymers has been reported to be effective at MWs above 100,000, where the increase in adhesive strength is proportional to MW due to the increased detachment force of high MW polymers onto the mucosal substrate. Consistently, the mucoadhesion of the CS-NPs increased with increasing cross-linker MW as described in the Materials section: TPP (367.9 Da), DS (15 kDa), AG (250 kDa), and HA (1000 kDa).

In addition to the numerous factors, higher mucoadhesive properties of CS-AG and CS-HA NPs were also well explained in terms of cross-linker concentration (Sosnik et al., 2014). Indeed, a previous study reported that low concentrations of the cross-linker polymer tends to be associated with a decreased number of penetrating polymer chains per unit volume of mucus, resulting in an unstable interaction between polymer and mucus, while more concentrated polymers lead to better adhesion (Salamat-Miller et al., 2005). In this study, CS-AG and CS-HA NPs were prepared with 0.8 mg/mL of each cross-linker, while the other cross-linkers were used at concentrations of 0.2 mg/mL to achieve a similar particle size. Therefore, an increase in the total number of functional groups of CS-AG and CS-HA NPs with increasing concentration of cross-linkers also appears to have contributed to the interaction of CS-NPs with mucus, resulting in high adhesion.

3.6. *Transcellular transport across a co-culture cell monolayer*

Time courses of the cumulative amounts of transported QUE across Caco-2 and HT-29 co-cultured monolayer depending on the types of CS-NPs are shown in Fig. 5a. In the first 30 min, the amount of transported free QUE (0.17 ± 0.01 μmol/L) was higher than the transported QUE within CS-NPs (0.04–0.09 μmol/L). The cell monolayer in this study was highly efficient model for expression of the small intestinal environment, consisted of Caco-2 cells, an absorptive type cell known to express a variety of small intestinal cell functions, and HT-29 cells that excrete mucin upon differentiation (Antunes et al., 2013). Since the mucosal layer is the pre-stage of intestinal absorption, CS-NPs can be absorbed into epithelial cells after pass through the mucin layer (Salatin & Yari Khosroushahi, 2017). Therefore, such interactions between CS-NPs and mucin likely improved the residence time at intestine, but also prolonged the passage of the mucosal layer, consequently reducing the amount of permeated QUE in the early stage (Bernkop-Schnürch, 2005).

However, the transportation of QUE from CS-AG and CS-HA NPs gradually increased over time, then the cumulative amount of transported QUE by (0.78 ± 0.09 μmol/L) and CS-HA NPs (0.80 ± 0.03 μmol/L) reached that of transported free QUE (0.79 ± 0.04 μmol/L) after 120 min. Since the transport flux expressed as slope of the cumulative amounts of total transported QUE, CS-AG (0.0083) and CS-HA NPs (0.0080) exhibited significantly higher transport flux compared with that of free QUE (0.0068). Moreover, since the apparent permeability coefficient (*P*app) was calculated using the transport flux, *P*app values according to the types of samples also exhibited that *P*app of free QUE (11.53 ± 0.60 cm^{-6}/s) was significantly increased by encapsulation within CS-AG (13.80 ± 0.24 cm^{-6}/s) and CS-HA NPs (13.24 ± 0.42 cm^{-6}/s) (Fig. 5b). This result can be explained that effective mucoadhesive properties of CS-NPs could improve time-dependent cell penetration of QUE in the mucosa-adherent state. Therefore, CS-AG and CS-HA NPs could promote cell permeation of QUE significantly entire permeation period, due to their efficient mucoadhesion properties as mentioned in the *in vitro* mucoadhesion study.

Conversely, CS-TPP (11.34 ± 0.59 cm^{-6}/s) and CS-DS NPs (10.61 ± 0.77 cm^{-6}/s) exhibited cell permeability similar to that of free QUE despite significantly higher mucoadhesion. This result may be explained by the stationary experimental condition of the cellular permeation

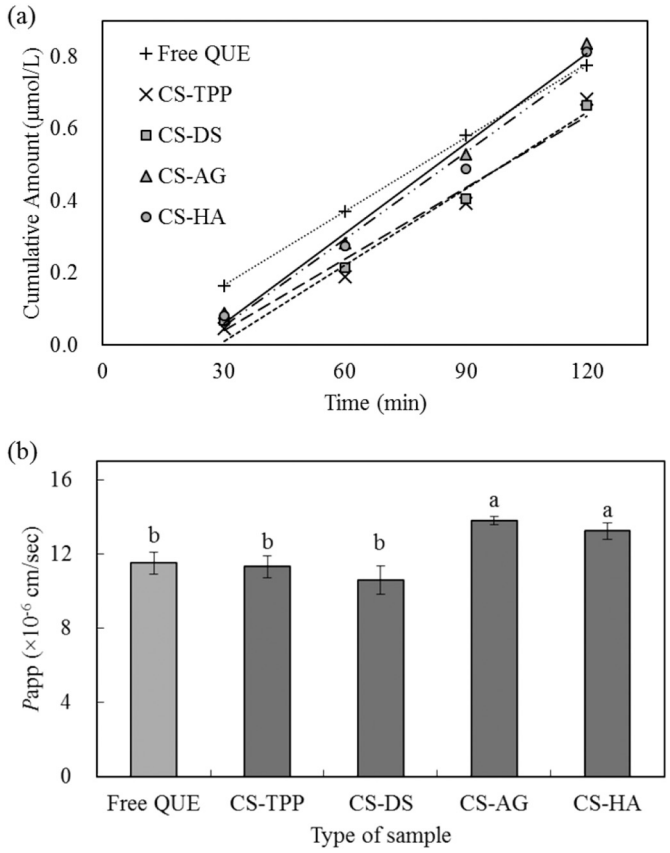

Fig. 5. Cell permeability through Caco-2 and HT-29 co-cultured cell monolayer: cumulative amounts (a) and apparent permeability coefficients (P_{app}) (b) of the free QUE and QUE from CS-NPs prepared with tripolyphosphate (TPP), dextran sulfate (DS), Arabic gum (AG), and hyaluronic acid (HA). Data are the mean of three replicates, and error bars indicate the standard deviation. [a–e]Means with different letters indicate significant difference ($p < 0.05$).

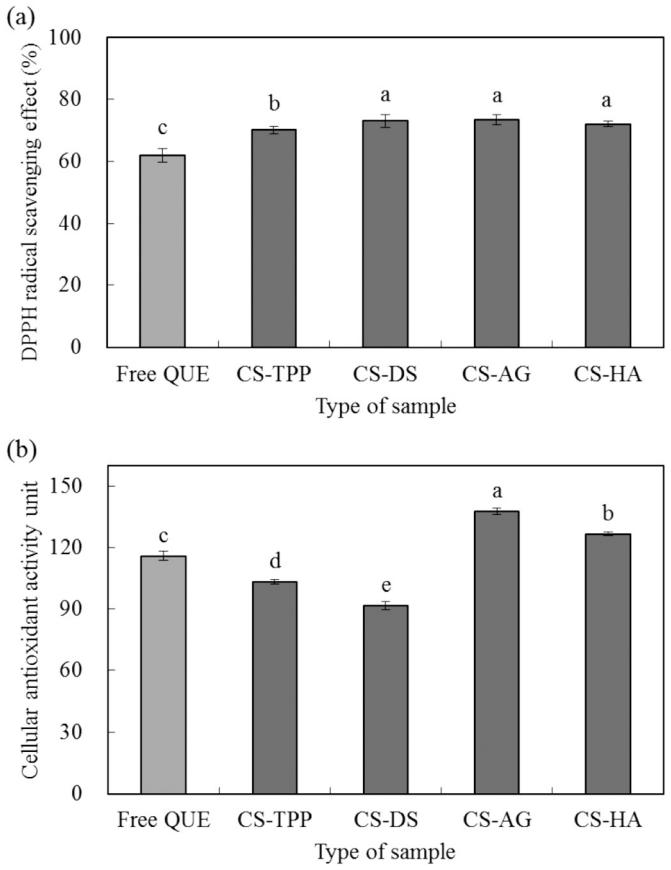

Fig. 6. *In vitro* DPPH radical scavenging (a) and cellular antioxidant activity in Caco-2 cells (b) of free QUE and QUE-loaded CS-NPs prepared with tripolyphosphate (TPP), dextran sulfate (DS), Arabic gum (AG), and hyaluronic acid (HA). Data are the mean of three replicates, and the error bars indicate the standard deviation. [a–c]Means with different letters are significantly different ($p < 0.05$).

assay. Cell attachment characteristics improve intestinal absorption of the ingested materials by increasing the residence time during dynamic migration along the gastrointestinal site. However, in the stationary experimental environment, it can be judged that the adhesion effects of CS-TPP and CS-DS NPs was less expressed due to their relatively weaker adhesion effects compared with the other CS-NPs.

3.7. *In vitro* DPPH radical scavenging

DPPH radical scavenging activity was assessed *in vitro* by evaluating the proton donating ability of free QUE and QUE-loaded CS-NPs prepared with different cross-linkers (Fig. 6a). The radical scavenging ability of free QUE was found to be 65.7 ± 3.5%, which was significantly increased by encapsulation within all types of CS-NPs (68.6–73.5%). Since antioxidant materials react with radicals in a dissolved state, material solubility is understood to be a key factor affecting the antioxidant activity *in vitro*. For example, a previous study reported that free radical scavenging capacity of kaempferol was significantly increased after encapsulation within CS-NPs due to increased aqueous solubility (Ilk et al., 2017). Likewise, because QUE has similar low aqueous solubility characteristics to kaempferol, its increased antioxidant activity appeared to be due to increased solubility through encapsulation. On the other hand, in this study, all of the CS-NPs were fabricated and evaluated at 60 μM of QUE, a concentration that was not cytotoxic as mentioned above. Indeed, at this concentration, QUE was relatively stable in solution and did not exhibit turbidity or form any precipitants. Therefore, the effects of increasing the solubility by encapsulation within CS-NPs were relatively weaker compared with previous studies aimed primarily toward solubility enhancement. Although CS-TPP NPs exhibited significantly lower radical scavenging activity compared to other CS-NPs, the large numerical difference in activity was not dependent on the type of CS-NPs. Particle size of NPs has been reported to be one of the major decisive factors affecting the solubility of NPs due to the increase in surface area with particle size reduction. The CS-NPs of this study were prepared such that they had similar particle sizes to allow for clear comparison of the different cross-linkers. Thus, the contribution of solubility on experimental variance due to physical particle size was decreased and revealed similar antioxidant activities among the different CS-NPs *in vitro*.

3.8. *Cellular antioxidant activity*

Measurement of cellular antioxidant activity can reflect various mechanisms that are not present during *in vitro* DPPH radical scavenging experiments (Wolfe & Liu, 2007). Therefore, the effects of CS-NPs on antioxidant activity should be more apparent in cellular antioxidant activity assays compared with *in vitro* DPPH radical scavenging assays. Moreover, because cellular antioxidant activity is expressed after permeation of antioxidant into target cells, the cellular antioxidant activity may reflect mucoadhesion and cell permeability studies. The cellular antioxidant activity of free QUE was 115.8 ± 4.4, and the activity was significantly increased within CS-AG and CS-HA NPs, with antioxidant activities of 137.5 ± 8.2 and 126.5 ± 8.1, respectively (Fig. 6b). As mentioned above, CS-AG and CS-HA NPs possess several features needed for effective cell permeation including positive charge,

high MW, and concentration of cross-linkers, which led to increased cellular antioxidant activity due to acceleration of QUE permeation into cells. On the other hand, the antioxidant activities of CS-TPP (103.3 ± 9.9) and CS-DS NPs (91.7 ± 8.4) were significantly lower than that of free QUE. This result also relevant the permeation study that CS-TPP and CS-DS NPs which exhibited significantly lower cell permeability than other CS-NPs. Moreover, QUE could be relatively freely permeable into cells without interaction with the cell membrane within a stationary experimental environment and, over a limited period of reaction time, may exhibit higher activity than that of CS-TPP and CS-DS NPs.

Compared with CS-TPP NPs, though CS-DS NPs exhibited similar cell permeability properties and higher *in vitro* mucoadhesion, cellular antioxidant activity of CS-DS was significantly lower than that of CS-TPP. This result can be interpreted in terms of QUE release behavior, whereby the rate of QUE release from CS-DS NPs was significantly lower than that of CS-TPP. Measurement of cellular antioxidant activity in this study consisted of treating cells with antioxidants and measuring the subsequent activity of the introduced antioxidants; thus, the antioxidants only exhibited activity after release from their respective CS-NPs (Chen et al., 2014). Therefore, the substantial release of QUE from CS-DS NPs after entering cells was less than that of CS-TPP NPs, may result in an overall decrease in cellular antioxidant activity over a limited period of reaction time.

4. Conclusions

QUE-loaded CS-NPs of similar particle size (461.2–468.1 nm) were prepared by ionic gelation between CS and the cross-linkers; TPP (367.9 Da), DS (15 kDa), AG (>250 kDa), or HA (>1000 kDa) at pH 3.5. Although each cross-linker practically has wide range of properties, the cross-linkers used in this study were selected as those with characteristics commonly used in the previous studies. Thus, our novel approach involving the use of identical preparation conditions could provide useful information regarding the effects of cross-linkers on CS-NPs properties.

MW and concentration of cross-linkers, and degree of positive charge of NPs according to ZP were all found to affect mucoadhesion and cell permeation of CS-NPs. In this study, CS-AG (0.44 ± 0.02 mg/mL) and CS-HA NPs (0.50 ± 0.03 mg/mL) prepared with cross-linkers of higher concentration (0.8 mg/mL) and MW exhibited a significantly higher degree of mucoadhesion compared with CS-TPP (0.33 ± 0.04 mg/mL) and CS-DS NPs (0.41 ± 0.05 mg/mL). This tendency was consistent with the results of a cell permeability analysis and verified in the cellular antioxidant experiments showing that higher mucoadhesion properties of CS-AG and CS-HA NPs accelerated the permeation of QUE into cells. The results suggest that CS-NPs prepared from higher MW cross-linkers and relatively high concentrations have acceptable NP characteristics and may be useful as effective oral delivery system aimed at improving the absorption of QUE. In addition, further confirmation studies will be necessary, such as *in vivo* studies that can be more effectively analyze delivery compared to the stationary conditions used in this study, where adhesion or permeation effects were reduced.

Declaration of interest

The authors state no conflict of interest.

CRediT authorship contribution statement

Eun Suh Kim: Investigation, Visualization, Writing – original draft, Writing – review & editing. **Da Young Kim:** Investigation, Writing – original draft. **Ji-Soo Lee:** Conceptualization, Investigation, Data curation. **Hyeon Gyu Lee:** Project administration, Supervision, Funding acquisition.

Acknowledgements

This work was supported by the National Research Foundation of Korea (NRF) grant funded by the Korea government (MSIT) (No. 2021R1A2C2013460).

References

Abd El-Ghaffar, M. A., Hashem, M. S., El-Awady, M. K., & Rabie, A. M. (2012). pH-sensitive sodium alginate hydrogels for riboflavin controlled release. *Carbohydrate Polymers, 89*(2), 667–675.

Agnihotri, S. A., Mallikarjuna, N. N., & Aminabhavi, T. M. (2004). Recent advances on chitosan based micro and nanoparticles in drug delivery. *Journal of Controlled Release, 100*(1), 5–28.

Akahane, T., Takeuchi, S., & Minakata, A. (1990). Conductimetric titration of polyelectrolytes having sulfate and carboxyl groups. *Polymer Bulletin, 24*(4), 437–444.

Akolade, J. O., Oloyede, H. O. B., & Onyenekwe, P. C. (2017). Encapsulation in chitosan-based polyelectrolyte complexes enhances antidiabetic activity of curcumin. *Journal of Functional Foods, 35*, 584–594.

Antunes, F., Andrade, F., Araújo, F., Ferreira, D., & Sarmento, B. (2013). Establishment of a triple co-culture in vitro cell models to study intestinal absorption of peptide drugs. *European Journal of Pharmaceutics and Biopharmaceutics, 83*(3), 427–435.

Bagre, A. P., Jain, K., & Jain, N. K. (2013). Alginate coated chitosan core shell nanoparticles for oral delivery of enoxaparin: In vitro and in vivo assessment. *International Journal of Pharmaceutics, 456*(1), 31–40.

Bernkop-Schnürch, A. (2005). Mucoadhesive systems in oral drug delivery. *Drug Discovery Today: Technologies, 2*(1), 83–87.

Boots, A. W., Haenen, G. R., & Bast, A. (2008). Health effects of quercetin: From antioxidant to nutraceutical. *European Journal of Pharmacology, 585*, 325–337.

Brand-Williams, W., Cuvelier, M. E., & Berset, C. (1995). Use of a free radical method to evaluate antioxidant activity. *LWT - Food Science and Technology, 28*(1), 25–30.

Butstraen, C., & Salaün, F. (2014). Preparation of microcapsules by complex coacervation of gum arabic and chitosan. *Carbohydrate Polymers, 99*(2), 608–616.

Caddeo, C., Díez-Sales, O., Pons, R., Carbone, C., Ennas, G., Puglisi, G., et al. (2016). Cross-linked chitosan/liposome hybrid system for the intestinal delivery of quercetin. *Journal of Colloid and Interface Science, 461*, 69–78.

Chen, M., He, X., Wang, K., He, D., Yang, S., Qiu, P., et al. (2014). A pH-responsive polymer/mesoporous silica nano-container linked through an acid cleavable linker for intracellular controlled release and tumor therapy in vivo. *Journal of Materials Chemistry B, 2*(4), 428–436.

Compton, S. J., & Jones, C. G. (1985). Mechanism of dye response and interference in the Bradford protein assay. *Analytical Biochemistry, 151*(2), 369–374.

Coskun, O., Kanter, M., Korkmaz, A., & Oter, S. (2005). Quercetin, a flavonoid antioxidant, prevents and protects streptozotocin-induced oxidative stress and β-cell damage in rat pancreas. *Pharmacological Research, 51*(2), 117–123.

Dan, N. (2016). Transport and release in nano-carriers for food applications. *Journal of Food Engineering, 175*, 136–144.

Fan, W., Yan, W., Xu, Z., & Ni, H. (2012). Formation mechanism of monodisperse, low molecular weight chitosan nanoparticles by ionic gelation technique. *Colloids and Surfaces B: Biointerfaces, 90*, 21–27.

Hollman, P. C., Van Trijp, J. M., Mengelers, M. J., De Vries, J. H., & Katan, M. B. (1997). Bioavailability of the dietary antioxidant flavonol quercetin in man. *Cancer Letters, 114*, 139–140.

Ilk, S., Sağlam, N., Özgen, M., & Korkusuz, F. (2017). Chitosan nanoparticles enhances the anti-quorum sensing activity of kaempferol. *International Journal of Biological Macromolecules, 94*, 653–662.

Jang, K.-I., & Lee, H. G. (2008). Stability of chitosan nanoparticles for L-ascorbic acid during heat treatment in aqueous solution. *Journal of Agricultural and Food Chemistry, 56*(6), 1936–1941.

Je, H. J., Kim, E. S., Lee, J.-S., & Lee, H. G. (2017). Release properties and cellular uptake in Caco-2 cells of size-controlled chitosan nanoparticles. *Journal of Agricultural and Food Chemistry, 65*(50), 10899–10906.

Kim, D.-Y., & Shin, W.-S. (2015). Unique characteristics of self-assembly of bovine serum albumin and fucoidan, an anionic sulfated polysaccharide, under various aqueous environments. *Food Hydrocolloids, 44*, 471–477.

Kim, O. Y., Lee, S. M., Do, H., Moon, J., Lee, K. H., Cha, Y. J., et al. (2012). Influence of quercetin-rich onion peel extracts on adipokine expression in the visceral adipose tissue of rats. *Phytotherapy Research, 26*(3), 432–437.

Kizilay, E., Kayitmazer, A. B., & Dubin, P. L. (2011). Complexation and coacervation of polyelectrolytes with oppositely charged colloids. *Advances in Colloid and Interface Science, 167*, 24–37.

Kumari, A., Yadav, S. K., Pakade, Y. B., Singh, B., & Yadav, S. C. (2010). Development of biodegradable nanoparticles for delivery of quercetin. *Colloids and Surfaces B: Biointerfaces, 80*(2), 184–192.

Lee, J.-S., Suh, J. W., Kim, E. S., & Lee, H. G. (2017). Preparation and characterization of mucoadhesive nanoparticles for enhancing cellular uptake of coenzyme Q10. *Journal of Agricultural and Food Chemistry, 65*(40), 8930–8937.

Liang, J., Yan, H., Puligundla, P., Gao, X., Zhou, Y., & Wan, X. (2017). Applications of chitosan nanoparticles to enhance absorption and bioavailability of tea polyphenols: A review. *Food Hydrocolloids, 69*, 286–292.

Luo, Y., & Wang, Q. (2013). Recent advances of chitosan and its derivatives for novel applications in food science. *Journal of Food Processing & Beverages, 1*(1), 1–13.

Luo, Y., & Wang, Q. (2014). Recent development of chitosan-based polyelectrolyte complexes with natural polysaccharides for drug delivery. *International Journal of Biological Macromolecules, 64*, 353–367.
Mounsey, J. S., O'Kennedy, B. T., Fenelon, M. A., & Brodkorb, A. (2008). The effect of heating on β-lactoglobulin–chitosan mixtures as influenced by pH and ionic strength. *Food Hydrocolloids, 22*(1), 65–73.
Murota, K., & Terao, J. (2003). Antioxidative flavonoid quercetin: Implication of its intestinal absorption and metabolism. *Archives of Biochemistry and Biophysics, 417*(1), 12–17.
Nidhin, M., Indumathy, R., Sreeram, K., & Nair, B. U. (2008). Synthesis of iron oxide nanoparticles of narrow size distribution on polysaccharide templates. *Bulletin of Materials Science, 31*(1), 93–96.
Nurunnabi, M., Revuri, V., Huh, K. M., & Lee, Y. (2017). Polysaccharide based nano/microformulation: an effective and versatile oral drug delivery system. In *Nanostructures for oral medicine* (pp. 409–433). Elsevier.
Racoviţă, S., Vasiliu, S., Popa, M., & Luca, C. (2009). Polysaccharides based on micro-and nanoparticles obtained by ionic gelation and their applications as drug delivery systems. *Revue Roumaine de Chimie, 54*(9), 709–718.
Raja, M. A. G., Katas, H., & Wen, T. J. (2015). Stability, intracellular delivery, and release of siRNA from chitosan nanoparticles using different cross-linkers. *PLoS One, 10*(6), Article e0128963.
Ramasamy, T., Tran, T. H., Cho, H. J., Kim, J. H., Kim, Y. I., Jeon, J. Y., et al. (2014). Chitosan-based polyelectrolyte complexes as potential nanoparticulate carriers: Physicochemical and biological characterization. *Pharmaceutical Research, 31*(5), 1302–1314.
Salamat-Miller, N., Chittchang, M., & Johnston, T. P. (2005). The use of mucoadhesive polymers in buccal drug delivery. *Advanced Drug Delivery Reviews, 57*(11), 1666–1691.
Salatin, S., & Yari Khosroushahi, A. (2017). Overviews on the cellular uptake mechanism of polysaccharide colloidal nanoparticles. *Journal of Cellular and Molecular Medicine, 21*(9), 1668–1686.
Sanguansri, P., & Augustin, M. A. (2006). Nanoscale materials development - A food industry perspective. *Trends in Food Science & Technology, 17*(10), 547–556.
Shim, H. R., Lee, J.-S., Nam, H. S., & Lee, H. G. (2016). Nanoencapsulation of synergistic combinations of acai berry concentrate to improve antioxidant stability. *Food Science and Biotechnology, 25*(6), 1597–1603.
Shu, X., Zhu, K., & Song, W. (2001). Novel pH-sensitive citrate cross-linked chitosan film for drug controlled release. *International Journal of Pharmaceutics, 212*(1), 19–28.
Sosnik, A., das Neves, J., & Sarmento, B. (2014). Mucoadhesive polymers in the design of nano-drug delivery systems for administration by non-parenteral routes: A review. *Progress in Polymer Science, 39*(12), 2030–2075.
Sozer, N., & Kokini, J. L. (2009). Nanotechnology and its applications in the food sector. *Trends in Biotechnology, 27*(2), 82–89.
Suh, J. W., Lee, J.-S., Ko, S., & Lee, H. G. (2016). Preparation and characterization of mucoadhesive buccal nanoparticles using chitosan and dextran sulfate. *Journal of Agricultural and Food Chemistry, 64*(26), 5384–5388.
Wan, H., Liu, D., Yu, X., Sun, H., & Li, Y. (2015). A Caco-2 cell-based quantitative antioxidant activity assay for antioxidants. *Food Chemistry, 175*(15), 601–608.
Wolfe, K. L., & Liu, R. H. (2007). Cellular antioxidant activity (CAA) assay for assessing antioxidants, foods, and dietary supplements. *Journal of Agricultural and Food Chemistry, 55*(22), 8896–8907.
Wu, J., Wang, Y., Yang, H., Liu, X., & Lu, Z. (2017). Preparation and biological activity studies of resveratrol loaded ionically cross-linked chitosan-TPP nanoparticles. *Carbohydrate Polymers, 175*, 170–177.
Yang, H.-C., & Hon, M.-H. (2009). The effect of the molecular weight of chitosan nanoparticles and its application on drug delivery. *Microchemical Journal, 92*(1), 87–91.
Yang, L., Gao, S., Asghar, S., Liu, G., Song, J., Wang, X., et al. (2015). Hyaluronic acid/chitosan nanoparticles for delivery of curcuminoid and its in vitro evaluation in glioma cells. *International Journal of Biological Macromolecules, 72*, 1391–1401.
Yin, L., Ding, J., He, C., Cui, L., Tang, C., & Yin, C. (2009). Drug permeability and mucoadhesion properties of thiolated trimethyl chitosan nanoparticles in oral insulin delivery. *Biomaterials, 30*(29), 5691–5700.
Zhang, Y., Yang, Y., Tang, K., Hu, X., & Zou, G. (2008). Physicochemical characterization and antioxidant activity of quercetin-loaded chitosan nanoparticles. *Journal of Applied Polymer Science, 107*(2), 891–897.